NASA TM X-315

TECHNICAL MEMORANDUM
X-315

RESEARCH ON BLUNT-FACED ENTRY CONFIGURATIONS AT ANGLES OF ATTACK BETWEEN 60° AND 90°

By William H. Phillips

Langley Research Center
Langley Field, Va.

[redacted]

NATIONAL AERONAUTICS AND SPACE ADMINISTRATION

WASHINGTON

September 1960

[redacted]

NATIONAL AERONAUTICS AND SPACE ADMINISTRATION

TECHNICAL MEMORANDUM X-315

RESEARCH ON BLUNT-FACED ENTRY CONFIGURATIONS AT ANGLES OF ATTACK BETWEEN 60° AND 90° *

By William H. Phillips

SUMMARY

This paper summarizes the aerodynamic characteristics and stability and control of reentry vehicles operating in the angle-of-attack range between 60° and 90°. Both capsule shapes and winged-reentry-type vehicles operating in this high angle-of-attack range are considered. A stable pitching-moment slope exists for the high angles of attack. However, a lack of aerodynamic damping makes stability augmentation necessary. By change in the blunt-face curvature both positive and negative lift-curve slopes can be obtained. Control can be obtained by vane-type flaps deflected to shift the centroid of area. The control effectiveness is good and reasonably linear for control deflections greater than 30° from the stream direction. It appears that at angles of attack near 90° the aerodynamic characteristics, which depend upon pressure forces on the front face, are predictable and independent of Mach number. Heat transfer and flow fields are difficult to predict but some experimental data are presented.

Author

INTRODUCTION

For entries into the atmosphere at small entry angles from low-altitude satellite orbits, blunt-faced nonlifting vehicles offer advantages of simplicity and minimum time of exposure to high heating conditions. An example of this type of vehicle is the Mercury capsule. A ballistic capsule, however, suffers from lack of maneuverability. Modification of the capsule design to incorporate provision for control of the angle of attack to produce lift allows reduction of peak deceleration and provides the possibility of control of the landing point. (See refs. 1 and 2.) A winged vehicle may also be designed to enter the atmosphere in the range of angle of attack from 60° to 90°. Some variable-geometry feature may be required to allow the vehicle to pitch down to conventional angles of attack for landing (ref. 3). The present paper summarizes the aerodynamic characteristics and stability and control of vehicles operating in this range.

*Title, Unclassified.

SYMBOLS

a_0 speed of sound at stagnation condition

C_D drag coefficient

C_L lift coefficient

$C_{L_\alpha} = \frac{dC_L}{d\alpha}$

C_m pitching-moment coefficient

$C_{m_q} = \frac{\partial C_m}{\partial \frac{qc}{2V}}$

$C_{m_\alpha} = \frac{dC_m}{d\alpha}$

C_X axial-force coefficient

$C_{X_\alpha} = \frac{dC_X}{d\alpha}$

c chord

$\bar{c}$ mean aerodynamic chord

c_p specific heat of fluid at constant pressure

h heat-transfer coefficient

L/D lift-drag ratio

M Mach number

M_α variation of pitching moment with angle of attack (presented about centroid of area)

M_∞ free-stream Mach number

N_{St} Stanton number, $\frac{h}{\rho V c_p}$

p pressure on wing surface

p_{MAX}	maximum pressure (at stagnation point)
q	dynamic pressure
R	Reynolds number; radius of disk
S	area
U	velocity at edge of boundary layer
$U_1, U_2, \ldots U_n$	specific values of velocity U
V	velocity
x	radial surface distance from center of disk (fig. 6)
α	angle of attack
$\frac{\alpha}{\alpha_0}$	ratio of amplitude of angle of attack to initial amplitude
δ_f	control-flap deflection
ρ	mass density

DISCUSSION

Aerodynamic Characteristics

The variations of lift, drag, and pitching-moment coefficients with angle of attack for a typical delta-wing configuration over the complete range of angle of attack from 0° to 90° are shown in figure 1. This figure indicates the range of conditions with which this paper is concerned and shows the typical variations that may be expected in this range. These data were obtained at a Mach number of 2, but similar trends would be indicated at other Mach numbers. The lift reaches a maximum in the neighborhood of 45° angle of attack and decreases to 0 at close to 90° angle of attack. The lift-curve slopes in the region considered in this paper, therefore, are negative. Simulator studies have shown that a pilot is capable of controlling a lifting vehicle in this region of negative lift-curve slope (refs. 4 and 5). As expected, the drag coefficient reaches its maximum value at 90° angle of attack. Pitching moments are herein presented about the centroid of area which produces a condition of trim at an angle of attack near 90°. For such a center-of-gravity location the vehicle is usually unstable at low angles of attack; however, it should be noted that the pitching-moment coefficient reaches a maximum and that a negative or stable slope exists between about 60° and 90° angle of attack.

[redacted]

Static Longitudinal Stability Characteristics

Basic longitudinal data on wings at an angle of attack of 90° are summarized in figure 2 for a variety of planforms. These results were taken from references 6 to 9 and from unpublished data. These planforms range from circular to a 75° sweptback delta. Planform has little effect on the characteristics provided the face is reasonably flat. The drag coefficient rises through the transonic range and reaches a fairly constant value beyond a Mach number of 2. A test point is given at a Mach number of 6.8 and another from the hot-shot tunnel of the Arnold Engineering Development Center at a Mach number of 18. These points confirm the fact that the drag coefficient does not vary much at hypersonic speeds. The lift-curve slope, when expressed per radian, may be shown to be equal to the negative of the drag coefficient plus the variation of axial-force coefficient with angle of attack. Contributions of the axial-force coefficient, however, are very small for flat wings, generally less than 2 percent of the value of the drag coefficient. For this reason the approximate value of the lift-curve slope per radian may also be read from the curve of drag coefficient by changing the sign. Values of static longitudinal stability C_{m_α} fall within the shaded region shown in figure 2. Most of the scatter is due to experimental error, because of the difficulty of measuring small pitching moments when the model is subjected to a large drag force. In spite of the experimental scatter, however, the variation of longitudinal stability with Mach number is shown to be much less than that usually experienced on conventional airplanes.

L 1 0 4 1

The aerodynamic characteristics shown in figure 1 are little affected by any design variation except that of varying the bluntness or curvature of the face. Effects of a wide variation in the face curvature are shown in figure 3. This figure includes data from a systematic series of capsule models tested at a Mach number of 6.8 and a number of winged vehicles. The value of static longitudinal stability C_{m_α} first increases with increased face rounding, and then decreases. These data are for a fixed location of the center of gravity with respect to the break line at the edge of the face. If the center of gravity were moved forward with increasing nose projection, the stability could be maintained. Increasing the curvature of the face first decreases the negative value and then produces a positive value of lift-curve slope. For capsules that are intended to be uncontrolled, a lift-curve slope near zero may be desired to reduce dispersion. For controllable devices, either the region of positive or negative lift-curve slope may be of interest. The values of L/D obtainable in either region of lift-curve slope are adequate for control of range and deceleration. Data for the winged vehicles are too near the origin to allow consistent determination of trends. These results show, however, that

[redacted]

small amounts of curvature may be incorporated in the lower surface of a winged vehicle without greatly affecting its aerodynamic characteristics at angles of attack near 90°.

Static Lateral Stability Characteristics

Lateral stability characteristics follow the same trends as longitudinal stability. The side force due to sideslip corresponds to the lift due to angle of attack, and the rolling moment due to sideslip corresponds to the pitching moment due to angle of attack. Tests have shown that these lateral stability derivatives are approximately constant in the range of angle of attack from 60° to 90°.

Flow Fields

Prediction of the detailed flow patterns on the faces of vehicles in the range approaching an angle of attack of 90° is of interest from the standpoint of aerodynamic heating and load distribution. A technique using small spots of oil on the face of the models has been utilized to trace the flow patterns on several configurations. Two such flow patterns are shown in figure 4, and corresponding schlieren pictures of the flow are shown in figure 5. A theory proposed by Mitchel H. Bertram and James C. Dunavant of the Langley Research Center, based on transformation of the known flow pattern on a circular disk, has been used to predict the streamlines at $\alpha = 90°$. This theory shows good agreement with experiment in the prediction of streamlines and pressure contours. The basis of the theory is shown in figure 6(a). A circle is inscribed in the planform, and three sets of lines parallel to the edges of the planform are drawn, with each set confined to the region between the center of the circle and the corresponding edge. In the regions where the sets of lines do not overlap (indicated by the shaded areas in fig. 6(a)), the velocities that would exist on a circular disk at any distance from the center are assumed to apply along each of the parallel lines passing through this point with the directions normal to the edge of the planform. In the regions where the sets of lines overlap, the velocity components associated with each set of lines are combined vectorially to obtain the resultant velocity at each point. The velocity as a function of radius for a circular disk is shown in figure 6(b).

As the angle of attack changes from 90° to 70° (fig. 5), the stagnation region moves rapidly forward from the centroid of the planform to the nose. Attempts are being made to predict the flow at angles of attack other than 90°, but as yet no good correlation with experiment has been obtained.

The schlieren pictures of figure 5 give an explanation of the static longitudinal stability exhibited by flat-faced configurations.

Newtonian flow theory would predict a constant pressure over the face at a given angle of attack and, therefore, no variation of pitching-moment coefficient with angle of attack would be expected. Actually, however, the curvature of the shock ahead of the wing produces a variation in pressure coefficient. The pressure is greater behind a normal shock than behind an oblique shock. As the angle of attack decreases from 90° to 70°, the shock near the nose becomes normal to the flow, whereas the shock inclination near the trailing edge decreases. Corresponding pressure changes on the face produce a stable variation of pitching-moment coefficient with angle of attack.

Heat Transfer

Measurements of heat transfer to the face of a 75° delta-wing model at a Mach number of 9.6 are shown in figure 7. These data show the variation of Stanton number with distance from the nose along the center line of the planform. Laminar-flow conditions existed in these tests. The spanwise variation of Stanton number is not shown, but, in general, the distribution across the span was fairly constant with a slight increase near the edges.

Simple analysis based on cross-flow theory, and ignoring the three-dimensional nature of the flow, would predict that the Stanton number would vary inversely as the square root of the width of the planform. The experimental data for 90° angle of attack show a much smaller variation than that predicted by this type of theory. Even at lower angles of attack, for which, as shown previously, the stagnation region moves rapidly to the nose, the variation along the center line is less than predicted by this theory. As a result, the heating in the critical region near the nose is reduced. More detailed calculations of the heat transfer at an angle of attack of 90°, based on the three-dimensional flow theory presented previously, have not yet been made, but good agreement with experiment, in the case of laminar flow, would be expected because of the agreement in predicting the flow pattern. Predictions at lower angles of attack are not possible until a suitable flow theory is developed.

Controls

Control of either a winged- or capsule-type vehicle in the high angle-of-attack range may be accomplished by means of vane-type controls hinged along the edges of the vehicle, which may be deflected to shift the centroid of area of the vehicle. Such controls may have their hinge lines located on the upper surface of the wing and set back from the edge to protect them from excessive aerodynamic heating. Typical locations for such controls are illustrated by the delta-wing configuration

in the upper left-hand corner of figure 8. In order to produce control about all three axes, the controls may be deflected in certain combinations. For example, the rear pair of controls on a delta-wing vehicle may be deflected differentially to produce rolling moments. The front pair may be deflected differentially to produce primarily yawing moments. Note that the yawing-moment requirements are small since the vehicle has no restoring moment in yaw in the high angle-of-attack range. The pitching moments may be produced by deflecting the front control alone or by differential deflection of the front and rear controls. The data available on the effect of control surfaces projecting from the edges of delta-wing configurations, capsules, and circular plates are indicated in the plots in figure 8. For controls deflected normal to the airflow, a correlation has been made showing the moment coefficient predicted on the basis of the shift of centroid of area as compared with that measured experimentally. As indicated by this curve these results are in good agreement. The variation of control effectiveness with control deflection has also been predicted by use of Newtonian flow concepts. The variation of control effectiveness with deflection for two controls is shown on the right-hand side of this figure. The results again indicate good prediction of the control effectiveness. Note that the controls produce little moment until they are deflected about 30° from the flow direction. Beyond this point, however, the control effectiveness shows a consistent and fairly linear variation.

Aerodynamic Damping

Aerodynamic damping of vehicles at angles of attack approaching 90° may be either stabilizing or destabilizing and is small in magnitude. Instability of longitudinal or lateral oscillations under conditions of constant dynamic pressure results from the negative lift-curve slope. On this instability is superimposed the well known tendency for the amplitude of oscillations to decrease in the region of increasing dynamic pressure and then to diverge in the region of decreasing dynamic pressure subsequent to the point of peak deceleration. Figure 9 shows this amplitude variation as a function of altitude during the entry. These results were obtained from the theoretical analysis of reference 10. This figure is for an uncontrolled vehicle, and the solid line represents the case with a value of C_{L_α} of -1.27 per radian and zero aerodynamic damping. The two additional curves indicate the effect of a more negative value of C_{L_α} and also of destabilizing C_{m_q}. Note that in the higher altitude range the aerodynamic characteristics have negligible effect and that the decrease in amplitude results solely from the increasing dynamic pressure. After the point of peak dynamic pressure the aerodynamic damping of an uncontrolled vehicle has a large effect on the amplitudes subsequently reached. The change in amplitude per cycle, however, even

for these rapid divergences, is relatively small. For example, the maximum change in amplitude per cycle in the worst case shown is only about 5 percent. Thus, only a small amount of artificial damping is required to stabilize the motion. Simulator studies of reference 4 have shown that this artificial damping is extremely desirable from the pilot's standpoint and, therefore, would probably be provided in any manned vehicle. In the absence of such damping, manual control of the oscillations is possible provided the period is sufficiently long.

CONCLUDING REMARKS

From the data presented, it appears that the aerodynamic characteristics of configurations at angles of attack approaching 90°, which depend on pressure forces on the front face, are predictable and relatively independent of Mach number in the range from zero to the highest Mach number for which test data are available. The static stability characteristics are good and control effectiveness of vane-type controls is linear and predictable. Lack of aerodynamic damping makes the provision of stability augmentation necessary. The three-dimensional nature of the flow makes accurate prediction of flow fields and heat transfer difficult. Experimental data are available, however, which provide a reasonably accurate basis for design. Although most of the available data are confined to the range below a Mach number of 4, the lack of dependence of the results on Reynolds number or on boundary-layer effects allows prediction of hypersonic characteristics with considerable confidence.

Langley Research Center,
National Aeronautics and Space Administration,
Langley Field, Va., April 11, 1960.

REFERENCES

1. Eggleston, John M., and Young, John W.: Trajectory Control for Vehicles Entering the Earth's Atmosphere at Small Flight-Path Angles. NASA MEMO 1-19-59L, 1959.

2. Cheatham, Donald C., Young, John W., and Eggleston, John M.: The Variation and Control of Range Traveled in the Atmosphere by a High-Drag Variable-Lift Entry Vehicle. NASA TN D-230, 1960.

3. Staff of Langley Flight Research Division (Compiled by Donald C. Cheatham): A Concept of a Manned Satellite Reentry Which Is Completed With a Glide Landing. NASA TM X-226, 1959.

4. Eggleston, John M., Baron, Sheldon, and Cheatham, Donald C.: Fixed-Base Simulation Study of a Pilot's Ability To Control a Winged-Satellite Vehicle During High-Drag Variable-Lift Entries. NASA TN D-228, 1960.

5. Assadourian, Arthur, and Cheatham, Donald C.: Longitudinal Range Control During the Atmospheric Phase of a Manned Satellite Reentry NASA TN D-253, 1960.

6. Spencer, Bernard, Jr.: An Investigation of the Aerodynamic Characteristics at Subsonic Speeds of a Nonlifting-Type Space-Capsule Model Simulating Escape and Reentry Configurations. NASA TM X-228 1960.

7. Penland, Jim A., and Armstrong, William O.: Static Longitudinal Aerodynamic Characteristics of Several Wing and Blunt-Body Shapes Applicable for Use as Reentry Configurations at a Mach Number of 6 and Angles of Attack up to 90°. NASA TM X-65, 1959.

8. Foster, Gerald V.: Exploratory Investigation at Mach Number of 2.01 of the Longitudinal Stability and Control Characteristics of a Winged Reentry Configuration. NASA TM X-178, 1959.

9. Ware, George M.: Low-Subsonic-Speed Static Longitudinal Stability and Control Characteristics of a Winged Reentry-Vehicle Configuration Having Wingtip Panels That Fold up for High-Drag Reentry. NASA TM X-227, 1960.

10. Lichtenstein, Jacob H.: Analytical Investigation of the Dynamic Behavior of a Nonlifting Manned Reentry Vehicle. NASA TN D-416, 1960.

L 1 0 4 1

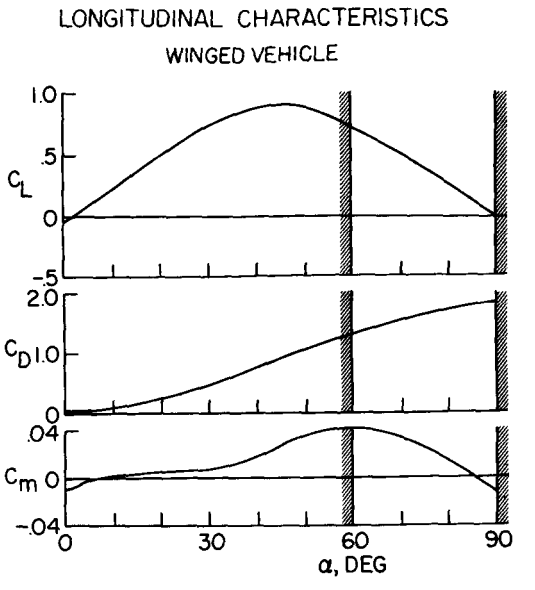

Figure 1

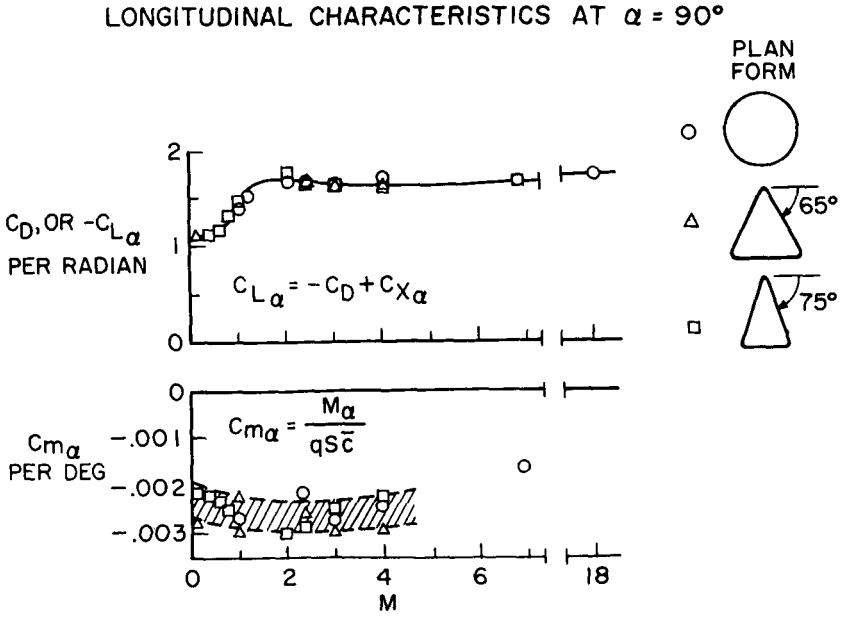

Figure 2

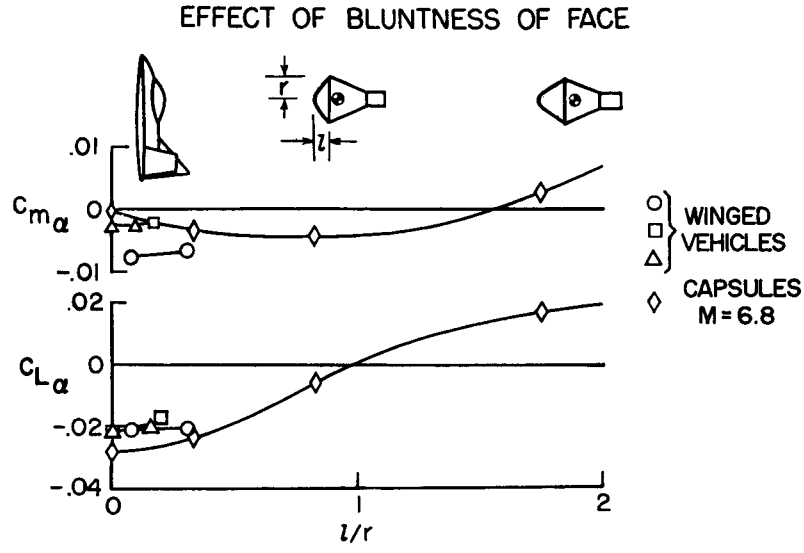

Figure 3

FLOW FIELDS ON DELTA WINGS AT HIGH ANGLE OF ATTACK

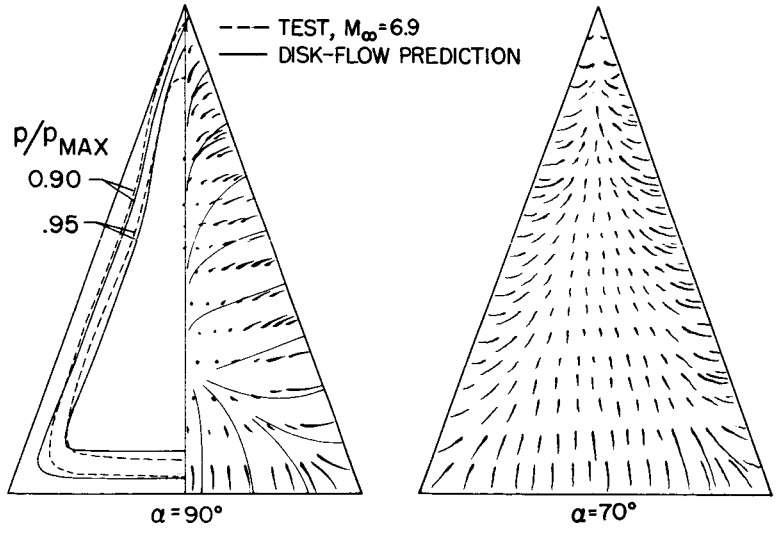

Figure 4

SCHLIEREN PHOTOGRAPHS OF FLOW

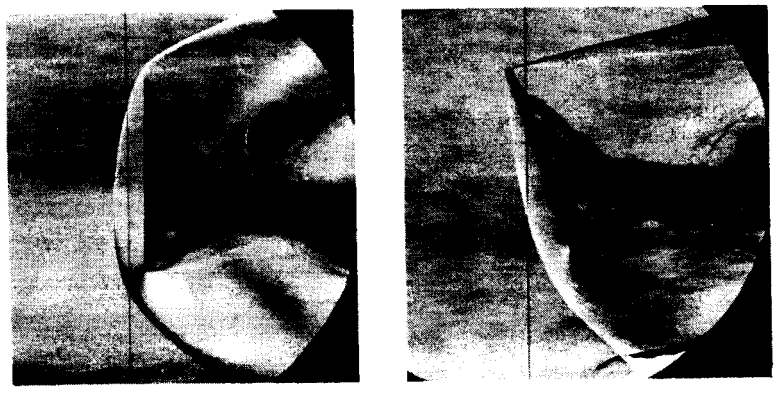

α=90° α=70°

L-60-2466

Figure 5

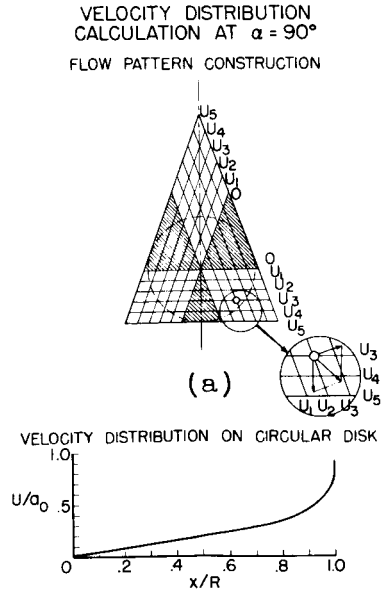

Figure 6

EXPERIMENTAL HEAT TRANSFER TO DELTA WING

M=9.6 ; R = 450,000 ; DATA TAKEN ALONG CENTER LINE

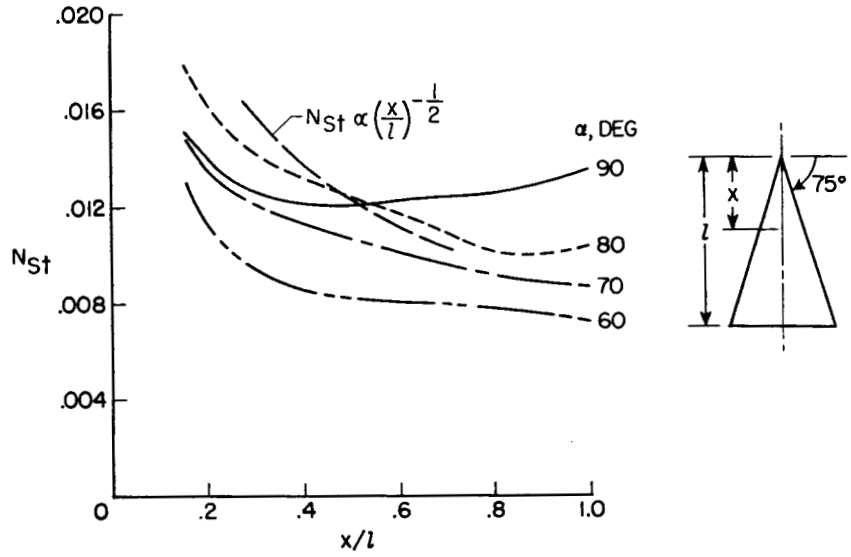

Figure 7

CONTROL-SURFACE EFFECTIVENESS

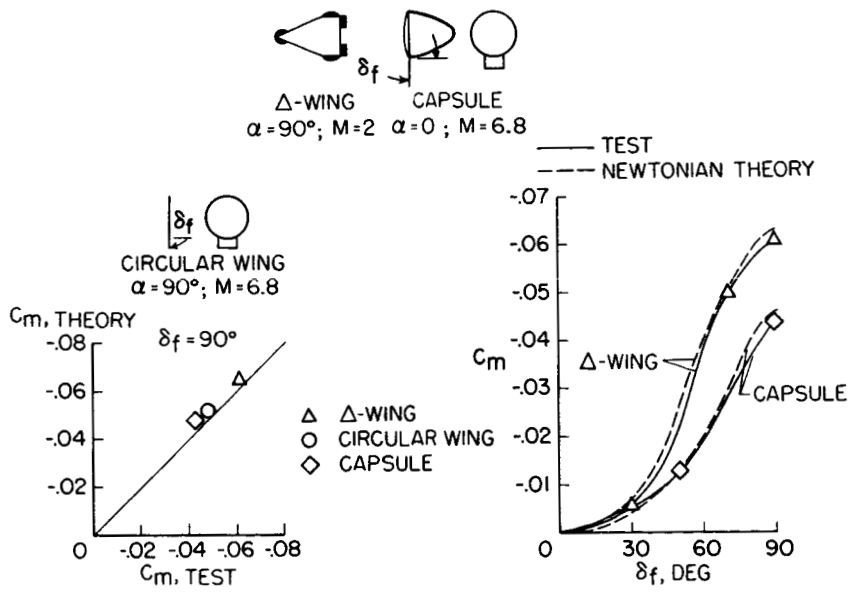

Figure 8

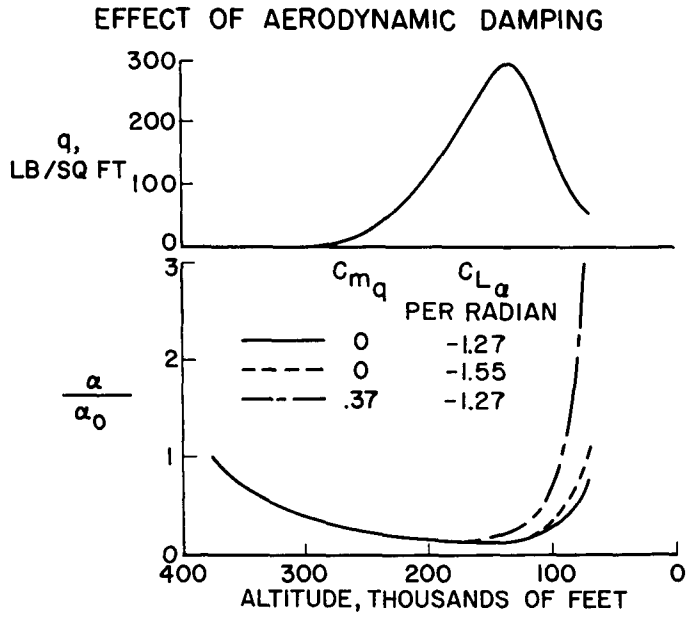
EFFECT OF AERODYNAMIC DAMPING
300
200
q,
LB/SQ FT
100
0
3
2
α
α0
1
0
C_{m_q}
C_{L_α}
PER RADIAN
0
-1.27
0
-1.55
.37
-1.27
400
300
200
100
0
ALTITUDE, THOUSANDS OF FEET

Figure 9